



## ISTITUTO NAZIONALE DI RICERCA METROLOGICA Repository Istituzionale

A method to deal with correlations affecting  $\gamma$  counting efficiencies in analytical chemistry measurements performed by  $k_0$ -NAA

This is the author's accepted version of the contribution published as:

*Original*

A method to deal with correlations affecting  $\gamma$  counting efficiencies in analytical chemistry measurements performed by  $k_0$ -NAA / DI LUZIO, Marco; D'Agostino, Giancarlo; Oddone, Massimo. - In: MEASUREMENT SCIENCE & TECHNOLOGY. - ISSN 0957-0233. - 31:7(2020), p. 074006. [10.1088/1361-6501/ab7ca8]

*Availability:*

This version is available at: 11696/62217 since: 2021-01-19T16:15:31Z

*Publisher:*

IOP

*Published*

DOI:10.1088/1361-6501/ab7ca8

*Terms of use:*

This article is made available under terms and conditions as specified in the corresponding bibliographic description in the repository

*Publisher copyright*

Institute of Physics Publishing Ltd (IOP)

IOP Publishing Ltd is not responsible for any errors or omissions in this version of the manuscript or any version derived from it. The Version of Record is available online at DOI indicated above

(Article begins on next page)

**Title:** A method to deal with correlations affecting  $\gamma$  counting efficiencies in analytical chemistry measurements performed by  $k_0$ -NAA

**Authors:** M. Di Luzio<sup>1</sup>, G. D'Agostino<sup>1</sup>, M. Oddone<sup>1,2</sup>

<sup>1</sup> c/o Unit of Radiochemistry and Spectroscopy, University of Pavia, Istituto Nazionale di Ricerca Metrologica (INRIM), via Taramelli 12, 27100 Pavia, Italy

<sup>2</sup> Department of Chemistry, University of Pavia, via Taramelli 12, 27100 Pavia, Italy

## Abstract

The ratio of  $\gamma$  counting efficiencies has predominant importance in trace element analysis carried out by prompt- and delayed- $\gamma$  neutron activation based on  $k_0$  standardization. Although the effect of correlation between counting efficiencies is well-known and methods have been developed and adopted in prompt- $\gamma$  neutron activation analysis to correctly evaluate the uncertainty, proposals and applications in delayed- $\gamma$  neutron activation analysis are still missing. To fill the gap, we developed a new method based on the use of reference  $\gamma$ -sources to determine the detection efficiency ratio and its uncertainty by taking full account correlations. A measurement model to some extent different from the classical  $k_0$  formulation widely used in delayed- $\gamma$  neutron activation analysis is required. A detection system was characterized to test the suitability of the method in a double-counting position setup, where the standard is placed far from and the sample is placed close to the detector end-cap. The present paper is a significant expansion over a relevant abstract presented at the “Mathematical and Statistical Methods for Metrology” Workshop, Torino, Italy, 30-31 May 2019 (pages 27-28 in <http://www.msmm2019.polito.it/programme>).

**Keywords:** correlations,  $\gamma$  counting efficiency, uncertainty, neutron activation analysis,  $k_0$  standardization

## Introduction

Counting efficiency of  $\gamma$ -ray detectors plays a key role in quantitative elemental analysis based on Prompt Gamma (neutron) Activation Analysis (PGAA) and (delayed gamma) Neutron Activation Analysis (NAA) [1].

In PGAA, sample irradiation and  $\gamma$  counting are simultaneous and the measured count rate is directly linked to the reaction rate per target nucleus of the investigated element via the number of target nuclei, i.e. the measurand, the (full-energy  $\gamma$ -peak) counting efficiency and the  $\gamma$ -emission probability. In NAA,  $\gamma$  counting follows sample irradiation and the measured count rate is indirectly linked to the reaction rate per target nucleus via the number of target nuclei, the counting efficiency and the  $\gamma$ -emission probability; the indirect link is established by differential activation-decay equations involving half-life times of the produced radionuclides whose solutions might not be simple when multiple activation-decay schemes are involved.

Even though PGAA and NAA would allow the development of “direct” primary methods for measurement of amount of substance via well-understood physical models, “ratio” primary methods are widely applied to reach measurement uncertainties required in trace element analysis [2]. At present, the most adopted standardization technique alternative to the (conventional) relative methodology is the so called  $k_0$ -standardization.

A detailed and comprehensive description of the  $k_0$  approach applied to PGAA and NAA can be found in [3] and [4], respectively. In both cases, the measurement equation includes a ratio of two counting efficiencies

at different  $\gamma$ -ray energies which is typically considered as one of the main contributors to the combined uncertainty.

The counting efficiency is usually determined by a mathematical function selected to model the full-energy  $\gamma$ -peak efficiency curve in a fixed position with respect to the detector. The parameters of the function along with their estimated variances and covariances are obtained in a least-square fitting of absolute and/or relative efficiency data points measured using reference  $\gamma$ -sources consisting of radionuclides with traceable activities and/or well-known  $\gamma$ -emission probabilities, respectively.

Therefore, any two counting efficiencies used to calculate the ratio are to some extent correlated because they are estimated using a mathematical function defined by the same parameters. This is a typical case of correlated input quantities affecting the combined uncertainty of the result discussed in the Guide to the expression of Uncertainty in Measurement [5]. For example, when two counting efficiencies are calculated at close lying  $\gamma$  energies the uncertainty of the corresponding ratio is overestimated if their correlation is neglected.

In  $k_0$ -PGAA, a fitting method based on use of orthogonal polynomials has been proposed and successfully applied to compute the counting efficiency and to evaluate its uncertainty [6]. The covariance between two counting efficiencies, i.e. their correlation degree, was calculated from the Hessian matrix and properly used to evaluate the uncertainty of the ratio as shown in [7]. In addition, a generalized formalism was presented and applied to make explicit the effect of efficiency correlations in the evaluation of the uncertainty of ratios and products of counting efficiencies [8].

In  $k_0$ -NAA, the first developers of the method introduced the concept of “effective” solid angle to convert a counting efficiency in reference conditions, i.e. referred to a point-like source located far from the detector, to a counting efficiency in geometric conditions, i.e. referred to an extended source located close to the detector. Accordingly, the measurement model included a ratio of counting efficiencies calculated in reference conditions coupled to a ratio of “effective” solid angles usually obtained by numerical integrations [4]. To the best of our knowledge, the effect of correlation is neglected by most of the  $k_0$ -NAA users, even in simple cases where the ratio of “effective” solid angles is the unity value.

A possible alternative to the use of orthogonal polynomials has been applied in activation cross section determinations to evaluate the uncertainty of the counting efficiency ratio involved in the measurement model [9]. A suitable efficiency function was adjusted to experimental data in a least square algorithm and the output covariance matrix of the fitting parameters was used to calculate the covariance of two counting efficiencies. The uncertainty of the corresponding ratio was computed according to fit for purpose equations (38) and (39) reported in [10] together with the underlying basic concepts adopted to propagate the uncertainty.

In this paper, we propose an original method in some way similar to that applied in activation cross section measurements but purposely developed for  $k_0$ -NAA to determine  $\gamma$  counting efficiency ratios without the use of orthogonal polynomials to evaluate the uncertainty.

Specifically, the need to evaluate the covariance between counting efficiencies is avoided by redefining each counting efficiency with the mathematical function modeling the efficiency versus  $\gamma$  energy curve as to include as input quantities the common fitting parameters and the  $\gamma$  energies. This makes the evaluation of the uncertainty of the ratio straightforward via the general-purpose equation (13) reported in [5] and here

adopted since the fitting parameters are still correlated. It is worth to note that variances and covariances values of the fitting parameters are directly calculated by the least-square fit.

In previous works [11,12] we accomplished to consider correlations in the case of single-counting position setups, i.e. when sample and standard are measured at the same distance from the detector. Here we extend the method to the most common double-counting position setup, i.e. when the standard is counted far and the sample close to the detector.

### Measurement model

Most  $k_0$ -NAA users adopt the well-established measurement model following the classical formulation of  $k_0$ -standardization reported in [4]. Although this option offers great experimental flexibility, the evaluation of uncertainty appears challenging because it requires to consider correlations among counting efficiencies and effective solid angles.

To make straightforward the evaluation of the uncertainty, we attempted to substitute the “effective” solid angle concept by introducing input parameters accounting for extended source geometries and  $\gamma$  self-absorption. Accordingly, we rearranged the classical measurement model formulation to quantify the analyte mass fraction in the sample,  $w_a$ , with respect to the monitor mass fraction in the standard,  $w_m$ , to:

$$w_a = \frac{C_{s,a}}{C_{s,m}} \frac{k_0 \text{Au}(m)}{k_0 \text{Au}(a)} \frac{G_{\text{th } m} + \frac{G_e m Q_0 m(\alpha)}{f}}{G_{\text{th } a} + \frac{G_e a Q_0 a(\alpha)}{f}} \frac{\varepsilon_{\text{std}}(E_m) (1 - \delta\varepsilon_{r m} \delta d_m)}{\varepsilon_{\text{sm}}(E_a) (1 - \delta\varepsilon_{r a} \delta d_a)} \frac{m_{\text{std}}}{m_{\text{sm}}} w_m, \quad (1)$$

where  $C_s$  is the full-energy  $\gamma$ -peak count rate at saturation,  $m$  is the mass,  $\varepsilon$  is the point-like source full-energy  $\gamma$ -peak detection efficiency at calibrated counting position,  $E$  is the energy of  $\gamma$ -photons,  $k_0$  is the kay-zero factor,  $G_{\text{th}}$  and  $G_e$  are the thermal and epithermal neutron self-shielding factors,  $Q_0$  is the resonance integral to thermal neutron cross section ratio,  $f$  is the thermal to epithermal neutron flux ratio,  $\alpha$  is the shaping factor of the epithermal neutron flux,  $\delta d$  is the (small and not exactly known) vertical distance between the calibrated and actual counting position, and  $\delta\varepsilon_r$  is the relative variation of the detection efficiency per unit of vertical distance. In (1), subscripts std and sm refer to the standard and sample, respectively, a and m refer to the analyte and monitor, respectively, and

$$C_s(E) = N_p \xi G_{\text{abs}} \kappa_g / (COI t_l SDC), \quad (2)$$

where  $N_p$  is the  $\gamma$ -peak net area,  $\xi$  is the excess counting loss correction factor,  $G_{\text{abs}}$  is the  $\gamma$  self-absorption correction factor,  $\kappa_g$  is the extended source geometry correction factor,  $COI$  is the true-coincidences correction factor,  $t_l$  is the live time of the detection system, and  $S = (1 - e^{-\lambda t_{\text{irr}}})$ ,  $D = e^{-\lambda t_d}$  and  $C = (1 - e^{-\lambda t_c}) / \lambda t_c$  are the saturation, decay and counting factors, respectively, with  $\lambda$  the decay constant,  $t_{\text{irr}}$  the irradiation time,  $t_d$  the decay time and  $t_c$  the (real) counting time [4]. A comprehensive overview with a description of the input parameters can be found elsewhere [11].

It is worth to point out that we also added in (1) the input parameters  $\delta d$  and  $\delta\varepsilon_r$  to account for the difference between a calibrated counting position, where point-like reference  $\gamma$ -sources are measured to obtain the counting efficiency versus  $\gamma$  energy, and actual counting position, where samples and standards are measured. Best results are obtained when actual counting positions of standard and sample are as close as possible to their respective calibrated positions. The uncertainty due to position errors during  $\gamma$  counting might be considered by measuring the  $\delta\varepsilon_r$  value and setting to zero the  $\delta d$  value with an uncertainty depending on the experimental conditions.

The present study focuses on the fourth factor on the right-hand side of (1), i.e. the ratio of counting efficiencies at calibrated counting positions,

$$k_{\varepsilon} = \frac{\varepsilon_{\text{std}}(E_{\text{m}})}{\varepsilon_{\text{sm}}(E_{\text{a}})}. \quad (3)$$

Hereafter, calibrated counting positions are considered.

Typically, the standard counting position is at large distance from the detector, where true-coincidences are negligible, while the sample counting position might be at close distance to allow the quantification in case of low amounts of analyte. Accordingly, we express  $k_{\varepsilon}$  as a product of two factors:

$$k_{\varepsilon} = k_{\varepsilon\Delta E} k_{\varepsilon\Delta d}, \quad (4)$$

where  $k_{\varepsilon\Delta E} = \frac{\varepsilon_{\text{std}}(E_{\text{m}})}{\varepsilon_{\text{std}}(E_{\text{a}})}$  and  $k_{\varepsilon\Delta d} = \frac{\varepsilon_{\text{std}}(E_{\text{a}})}{\varepsilon_{\text{sm}}(E_{\text{a}})}$  independently describe the effect of a different  $\gamma$ -energy,  $\Delta E$ , of monitor and analyte at the standard counting position, and the effect of a different counting position distance,  $\Delta d$ , of standard and sample at the analyte  $\gamma$ -energy, respectively. From a mathematical point of view, (4) is equivalent to (3) multiplied by  $\frac{\varepsilon_{\text{std}}(E_{\text{a}})}{\varepsilon_{\text{std}}(E_{\text{a}})}$ .

The efficiency function we adopted to model  $\varepsilon$  versus  $E$  at the standard counting position,  $\varepsilon_{\text{std}}(E)$ , is the exponential of a six term polynomial (see [13], equation (9.5), for details),

$$\varepsilon_{\text{std}}(E) = e^{\sum_{i=1}^6 A_i E^{2-i}}. \quad (5)$$

To determine parameters  $A_1, A_2, A_3, A_4, A_5$  and  $A_6$ , and the corresponding covariance matrix we fitted in a least square algorithm the natural logarithm of (5) to the natural logarithm of  $\varepsilon_{\text{std}}(E_{\text{r}})$  data collected at different  $\gamma$ -energies  $E_{\text{r}}$  with reference  $\gamma$  sources counted at the standard counting position. The formula used to compute  $\varepsilon_{\text{std}}(E_{\text{r}})$  is

$$\varepsilon_{\text{std}}(E_{\text{r}}) = \frac{C_{\text{std}}(E_{\text{r}})}{A \Gamma}, \quad (6)$$

where  $A$  is the (traceable) activity of the  $\gamma$ -emitting radionuclide at the reference time,  $\Gamma$  is the  $\gamma$ -emission probability and

$$C(E_{\text{r}}) = N_{\text{p}} \xi / (COI \ t_1 \ DC) \quad (7)$$

is the full-energy  $\gamma$ -peak counting rate at the reference time.

Counting efficiencies in (3) might be normalized without changing the efficiency ratio value. Therefore, the use of a single radionuclide with well-known  $\Gamma$  values and unknown activity might be possible. Nevertheless, to maximize the number of fitting points, it is common practice to merge counting efficiencies data collected with traceable and non-traceable activities by adding the latter ones to the fitting parameters.

The explicit form of the  $k_{\varepsilon\Delta E}$  factor based on the efficiency function (5) and computed at  $E_{\text{m}}$  and  $E_{\text{a}}$  is

$$k_{\varepsilon\Delta E} = e^{\sum_{i=1}^6 A_i (E_{\text{m}}^{2-i} - E_{\text{a}}^{2-i})}. \quad (8)$$

In agreement with (5), the equation we adopted to model  $k_{\varepsilon\Delta d}$  versus  $E_{\text{a}}$  is the exponential of a six term polynomial:

$$k_{\varepsilon\Delta d}(E_a) = e^{\sum_{i=1}^6 B_i E_a^{2-i}}. \quad (9)$$

To determine parameters  $B_1, B_2, B_3, B_4, B_5$  and  $B_6$ , and the corresponding covariance matrix we fitted the natural logarithm of (9) to the natural logarithm of the standard to sample efficiency ratio data,

$$\frac{\varepsilon_{\text{std}}(E_r)}{\varepsilon_{\text{sm}}(E_r)} = \frac{C_{\text{std}}(E_r)}{C_{\text{sm}}(E_r)}, \quad (10)$$

where  $C_{\text{std}}(E_r)$  and  $C_{\text{sm}}(E_r)$  are the full-energy  $\gamma$ -peak count rates computed with (7), referred at the same fixed time and obtained with reference  $\gamma$ -sources counted at standard and sample counting positions.

To sum up, the measurement model for the ratio of counting efficiencies obtained from (8) and (9) is

$$k_{\varepsilon} = e^{\sum_{i=1}^6 A_i (E_m^{2-i} - E_a^{2-i}) + B_i E_a^{2-i}}, \quad (11)$$

where  $A_i, B_i, E_a$  and  $E_m$  are input parameters.

The redefinition of  $k_{\varepsilon}$  via (11) by-passes the need to evaluate the correlations between counting efficiencies because the uncertainty of  $k_{\varepsilon}$  can be directly computed according to equation (13) reported in [5] using variances and covariances of input fitting parameters  $A_i, B_i$  and  $\gamma$  energies.

Reference sources are typically counted until the uncertainty due to statistics of  $N_p$  reaches the sub-percent level. Therefore, besides equation model errors, major contributors to the uncertainty of  $k_{\varepsilon\Delta E}$  are expected to be the certified  $\gamma$ -emission rates of the reference sources, depending on their activities and  $\gamma$ -emission probabilities. On the other hand, since  $\gamma$ -emission rates are not required in (10), the main contributor to the uncertainty of  $k_{\varepsilon\Delta d}$  is counting statistics. This makes  $k_{\varepsilon\Delta E}$  independent on  $k_{\varepsilon\Delta d}$  and limits the information required to evaluate the uncertainty of  $k_{\varepsilon}$  to the covariances matrices of  $A_i$  and  $B_j$ .

In case of single-counting setups  $k_{\varepsilon} = k_{\varepsilon\Delta E}$  with uncertainty depending on the covariance matrix of  $A_i$ .

In addition, it is worth to note that the proposed method is also suitable for relative-NAA, both in double-counting and single-counting setups. In the first case  $k_{\varepsilon} = k_{\varepsilon\Delta d}$  with uncertainty depending on the covariance matrix of  $B_i$  while in the latter case  $k_{\varepsilon} = 1$  with zero uncertainty [11].

## Experimental

The detection system used in this study consisted of a coaxial high purity germanium (HPGe) detector CANBERRA GC3518 (relative efficiency 35%, resolution 1.8 keV FWHM at 1332 keV) connected to an ORTEC DSPEC 502 digital signal processor. The ORTEC Gamma Vision software (version 6.08) running on personal computer managed the DSPEC 502 and stored the collected  $\gamma$ -spectra.

Counting  $\gamma$ -spectra were collected using three multi- $\gamma$  sources, 3 mm diameter solid ring, containing (i)  $^{241}\text{Am}$ ,  $^{109}\text{Cd}$ ,  $^{57}\text{Co}$ ,  $^{139}\text{Ce}$ ,  $^{52}\text{Cr}$ ,  $^{113}\text{Sn}$ ,  $^{85}\text{Sr}$ ,  $^{137}\text{Cs}$ ,  $^{54}\text{Mn}$ ,  $^{88}\text{Y}$ ,  $^{65}\text{Zn}$  and  $^{60}\text{Co}$  (LEA, code 12ML01EGMA15), (ii)  $^{152}\text{Eu}$  (LEA, code EU152EGMA20) and (iii)  $^{133}\text{Ba}$  (LEA, code BA133EGMA20). Relative uncertainties ( $k = 1$ ) of the certified  $\gamma$ -emission rates are close to 2% with the exception of 3% for  $^{109}\text{Cd}$  88.03 keV in the case of (i), and to 1.5% with the exception of 3% for  $^{152}\text{Eu}$  563.99 keV and  $^{133}\text{Ba}$  53.16 keV in the case of (ii) and (iii), respectively. The  $E_r$  values assigned to  $\gamma$ -energies were retrieved from the corresponding multi- $\gamma$  source certificates and rounded to the second decimal digit as their uncertainties were negligible for this aim.

Aiming at applying (1) in  $k_0$ -NAA measurements, we fully characterized the detection system by establishing nine calibrated counting positions where the ratio of efficiencies can be obtained according to (3). Distances from the detector end-cap are shown in Figure 1.

The standard counting position was located at 18 cm using a polyethylene holder. Consecutive measurements of (i), (ii) and (iii) were performed by adjusting counting times to reach a statistical relative uncertainty lower than 0.5% for all  $\gamma$ -emissions, with the exception of 1.4% and 1.0% for the  $^{241}\text{Am}$  59.54 keV and  $^{133}\text{Ba}$  53.16 keV, respectively.

Eight equally spaced sample counting positions were placed using polyethylene holders each 2 cm, starting from 16 cm to 2 cm towards the detector end-cap. Consecutive measurements of (i) were performed at all counting positions by adjusting counting times to reach a statistical relative uncertainty lower than 0.5% for the true-coincidences free  $\gamma$ -emissions  $^{241}\text{Am}$  59.54 keV,  $^{109}\text{Cd}$  88.03 keV,  $^{57}\text{Co}$  122.06 keV,  $^{139}\text{Ce}$  165.86 keV,  $^{51}\text{Cr}$  320.08 keV,  $^{113}\text{Sn}$  391.70 keV,  $^{85}\text{Sr}$  514.00 keV,  $^{137}\text{Cs}$  661.66 keV,  $^{54}\text{Mn}$  834.85 keV and  $^{65}\text{Zn}$  1115.54 keV. True-coincidences  $\gamma$ -emissions were rejected because they require additional corrections when counted close to the detector end-cap. This limited the calibrated energy range between 59.54-1115.54 keV.

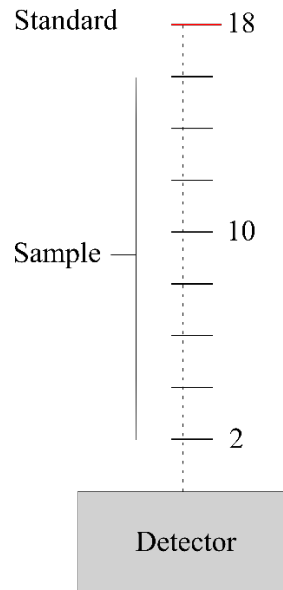


**Figure 1** Distances, in cm, of the calibrated counting positions from the detector end-cap. The eight positions assigned to the sample and the single position assigned to the standard are indicated.

The highest relative dead time, 11%, occurred during the counting of (ii) at 18 cm whereas during countings of (i) at the sample positions the maximum relative dead time, 5%, was reached at 2 cm.

## Results and discussion

The collected  $\gamma$ -spectra were elaborated with the HyperLab software to obtain  $N_p$ . Default settings were used to fit  $\gamma$ -peaks without manual adjustment of the parameters with the exception of the  $^{85}\text{Sr}$  514.00 keV peak close to the 511 keV annihilation peak and the  $^{133}\text{Ba}$  53.16 keV,  $^{241}\text{Am}$  59.54 keV,  $^{133}\text{Ba}$  79.61 keV and  $^{133}\text{Ba}$  81.00 keV peaks at the x-ray emissions region.

A total of 44  $\gamma$ -energies  $E_r$  (14 from the 12ML01EGMA15 multi- $\gamma$  source, 21 from the EU152EGMA20 and 9 from the BA133EGMA20) ranging from 53.16 keV to 1836.07 keV were used to compute  $\varepsilon_{\text{std}}(E_r)$  according to (6). The  $^{109}\text{Cd}$  88.03 keV,  $^{152}\text{Eu}$  563.99 keV and  $^{152}\text{Eu}$  1005.27 keV  $\gamma$ -emissions were rejected. Half-life times and  $\gamma$ -emission probabilities were retrieved from the nudat2 database [14] and the multi- $\gamma$  source certificates, respectively. The certified activity values of the radionuclides in 12ML01EGMA15 were adopted whereas the activities of  $^{152}\text{Eu}$  and  $^{133}\text{Ba}$  were considered unknown.

The natural logarithm of (5) was fitted to the natural logarithm of  $\varepsilon_{\text{std}}(E_r)$  values to obtain the parameters  $A_1, A_2, A_3, A_4, A_5$  and  $A_6$ , with the corresponding covariance matrix; resulting  $A_i$  parameters and correlation matrix are reported in Table 1a and Table 1b, respectively. To account for the unknown activities of  $^{152}\text{Eu}$  and  $^{133}\text{Ba}$ , we included two additional fitting parameters in the least square algorithm.

**Table 1** Parameters  $A_1, A_2, A_3, A_4, A_5$  and  $A_6$  of the efficiency function fitted at the standard counting position (a) and the corresponding correlation matrix (b). Values in parentheses indicate the standard ( $k = 1$ ) uncertainty and refer to the corresponding last digits.

(a)	$x_i$	(b)	$A_1$	$A_2$	$A_3$	$A_4$	$A_5$	$A_6$
$A_1 / \text{MeV}^{-1}$	-0.314(14)	$A_1$	1.000	-0.973	0.909	-0.833	0.764	-0.708
$A_2 / 1$	-7.286(29)	$A_2$	-0.973	1.000	-0.964	-0.904	-0.843	0.789
$A_3 / \text{MeV}$	0.450(14)	$A_3$	0.909	-0.964	1.000	-0.980	0.939	-0.896
$A_4 / \text{MeV}^2$	-0.0528(26)	$A_4$	-0.833	-0.904	-0.980	1.000	-0.988	0.963
$A_5 / \text{MeV}^3$	$2.31(19) \times 10^{-3}$	$A_5$	0.764	-0.843	0.939	-0.988	1.000	-0.993
$A_6 / \text{MeV}^4$	$-4.60(50) \times 10^{-5}$	$A_6$	-0.708	0.789	-0.896	0.963	-0.993	1.000

The efficiency function (5),  $\varepsilon_{\text{std}}(E)$ , fitted to the  $\varepsilon_{\text{std}}(E_r)$  values at the standard counting position and relative residuals are plotted in Figure 2a and Figure 2b, respectively. In figure 2b, dashed horizontal lines correspond to the expanded ( $k = 2$ ) uncertainty of  $\varepsilon_{\text{std}}(E)$  obtained by taking into account correlations while vertical error bars indicate the expanded ( $k = 2$ ) uncertainty of  $\varepsilon_{\text{std}}(E_r)$ , mainly due to certified activities and  $\gamma$ -emission probabilities.



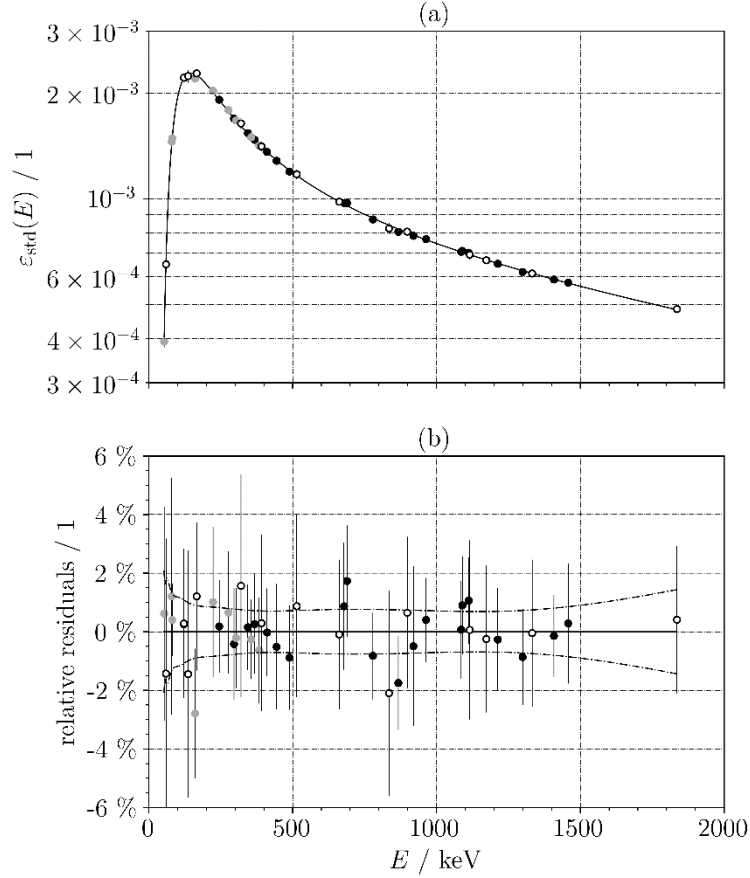


**Figure 2** The efficiency function at the standard counting position,  $\varepsilon_{\text{std}}(E)$ , fitted to the  $\varepsilon_{\text{std}}(E_r)$  values (a), and relative residuals (b) within the range 53.16-1836.07 keV;  $\varepsilon_{\text{std}}(E_r)$  values obtained with the 12ML01EGMA15, EU152EGMA20 and BA133EGMA20 multi- $\gamma$  sources are represented by hollow circles, black solid circles and gray solid circles, respectively. Dashed horizontal lines and vertical error bars correspond to the expanded ( $k = 2$ ) uncertainty of  $\varepsilon_{\text{std}}(E)$  and of  $\varepsilon_{\text{std}}(E_r)$ , respectively.

The overall well agreement between the experimental data and the fitted efficiency function is confirmed by the 2% scattering of relative residuals in Figure 2b.

The 10 true-coincidence free  $\gamma$ -energies  $E_r$  from the 12ML01EGMA15 multi- $\gamma$  source ranging from 59.54 keV to 1115.54 keV were used to compute  $\frac{\varepsilon_{\text{std}}(E_r)}{\varepsilon_{\text{sm}}(E_r)}$  according to (10) at the eight sample counting positions shown in Figure 1.

Equation (9) short of the parameter  $B_3$  was fitted to the natural logarithm of the  $\frac{\varepsilon_{\text{std}}(E_r)}{\varepsilon_{\text{sm}}(E_r)}$  values after transformation to natural logarithm to obtain parameters  $B_1, B_2, B_4, B_5$  and  $B_6$ , with the corresponding covariance matrix. The parameter  $B_3$  was deleted because, in a first fitting attempt, it was found to be statistically non-significant in all sample counting positions ( $P$  values higher than 0.11).

Fitted  $k_{\varepsilon\Delta d}$  functions and  $\frac{\varepsilon_{\text{std}}(E_r)}{\varepsilon_{\text{sm}}(E_r)}$  values at the eight sample counting positions are plotted in Figure 3; vertical error bars, somewhere visible, indicate the expanded ( $k = 2$ ) uncertainty due to counting statistics.

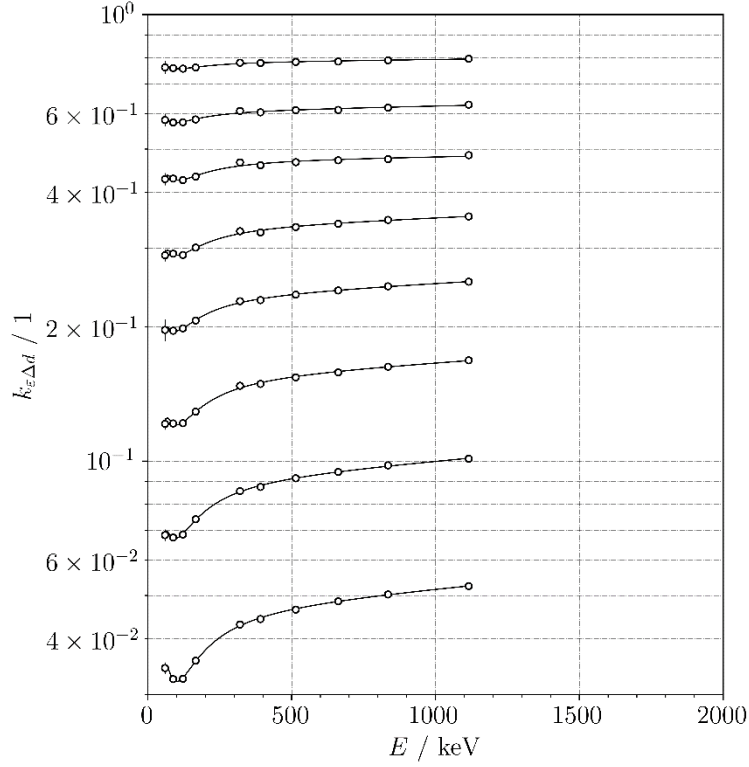


**Figure 3** Fitted  $k_{\epsilon\Delta d}$  functions and  $\frac{\epsilon_{std}(E_r)}{\epsilon_{sm}(E_r)}$  values obtained within the range 59.54-1115.54 keV at the eight sample counting positions with the true-coincidence free  $\gamma$ -emissions of the 12ML01EGMA15 multi- $\gamma$  source. Functions are plotted in vertical descending order from 16 cm to 2 cm distance from the detector end-cap. Vertical error bars, somewhere visible, correspond to the expanded ( $k = 2$ ) uncertainty.

Parameters  $B_i$  and the correlation matrix obtained at 2 cm sample position are reported in Table 2a and Table 2b, respectively. The corresponding  $k_{\epsilon\Delta d}$  function fitted to  $\frac{\epsilon_{std}(E_r)}{\epsilon_{sm}(E_r)}$  values, and relative residuals are plotted in Figure 4a and Figure 4b, respectively. In Figure 4b, the dashed horizontal lines correspond to the expanded ( $k = 2$ ) uncertainty of  $k_{\epsilon\Delta d}$  obtained by taking into account correlations while the vertical error bars indicate the expanded ( $k = 2$ ) uncertainty due to counting statistics.

**Table 2.** Parameters  $B_1, B_2, B_4, B_5$  and  $B_6$  of the fitted  $k_{\epsilon\Delta d}(E_a)$  function at 2 cm from the detector end-cap (a) and the corresponding correlation matrix (b). Values in parentheses indicate the standard ( $k = 1$ ) uncertainty and refer to the corresponding last digits.

(a)	$x_i$	(b)	$B_1$	$B_2$	$B_4$	$B_5$	$B_6$
$B_1 / \text{MeV}^{-1}$	0.132(10)	$B_1$	1.000	-0.951	0.743	-0.678	0.636
$B_2 / 1$	-3.081(12)	$B_2$	-0.951	1.000	-0.846	0.785	-0.743
$B_4 / \text{MeV}^2$	$-1.680(67) \times 10^{-2}$	$B_4$	0.743	-0.846	1.000	-0.991	0.975
$B_5 / \text{MeV}^3$	$1.853(93) \times 10^{-3}$	$B_5$	-0.678	0.785	-0.991	1.000	-0.996
$B_6 / \text{MeV}^4$	$-5.50(33) \times 10^{-5}$	$B_6$	0.636	-0.743	0.975	-0.996	1.000

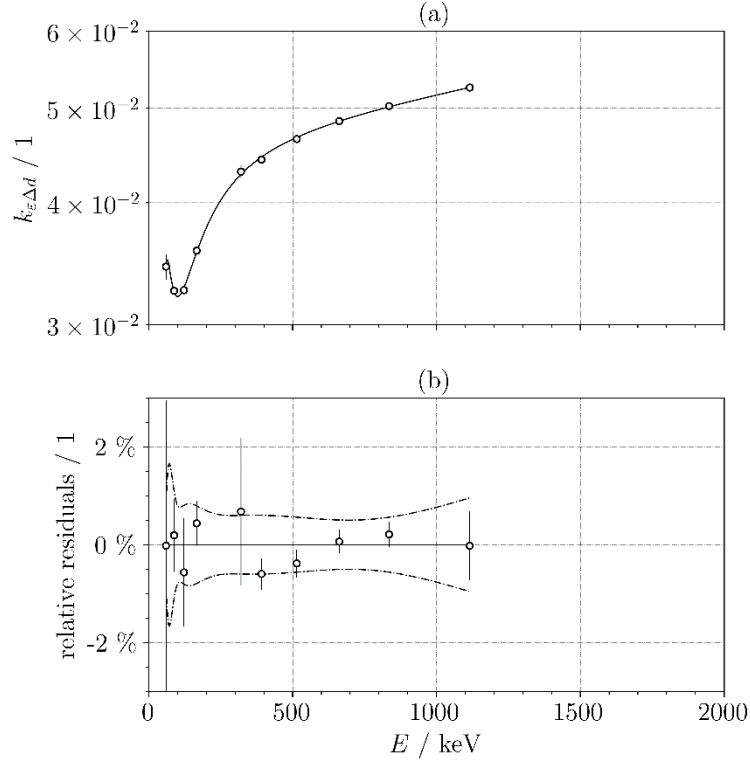


**Figure 4** Fitted  $k_{\epsilon\Delta d}$  function and  $\frac{\epsilon_{\text{std}}(E_r)}{\epsilon_{\text{sm}}(E_r)}$  values within the range 59.54-1115.54 keV at 2 cm distance from the detector end-cap (a), and relative residuals (b). Dashed horizontal lines and vertical error bars correspond to the expanded ( $k = 2$ ) uncertainty of  $k_{\epsilon\Delta d}$  and of  $\frac{\epsilon_{\text{std}}(E_r)}{\epsilon_{\text{sm}}(E_r)}$ , respectively.

The least square algorithm always succeeded in fitting the data without showing instabilities that would require the use of orthogonal polynomials.

As an example, we calculate and report here the  $k_{\epsilon}$  value for the determination of a nonspecific analyte in a sample performed by counting  $\gamma$ -photons emitted at energy  $E_a$  using the  $^{198}\text{Au}$  411.8 keV  $E_m$   $\gamma$ -emission as a monitor in a standard. We refer to a double-counting position setup with sample and standard measured at 2 cm and 18 cm from the detector end-cap, respectively.

The  $k_{\epsilon\Delta E}$  function computed with (8) and the corresponding relative expanded ( $k = 2$ ) uncertainty,  $U_r(k_{\epsilon\Delta E})$ , are plotted versus  $E_a$  in Figure 5a and Figure 5b, respectively. As expected at 411.8 keV  $\gamma$ -energy,  $k_{\epsilon\Delta E} = 1$  with zero uncertainty as a result of correlations between the parameters  $A_1, A_2, A_3, A_4, A_5$  and  $A_6$ .

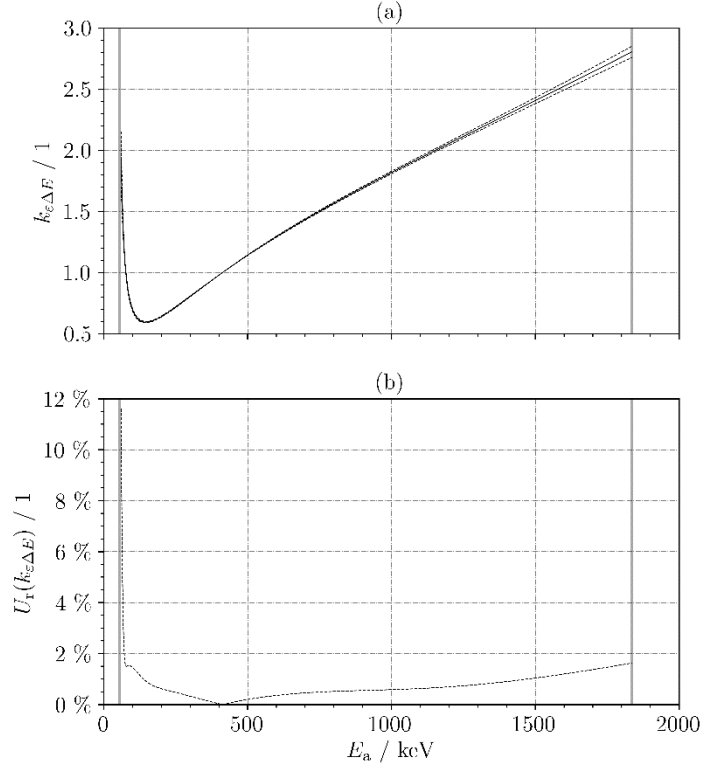


**Figure 5** The  $k_{\epsilon\Delta E}$  function (a) and the corresponding relative expanded ( $k = 2$ ) uncertainty,  $U_r(k_{\epsilon\Delta E})$ , (b) versus  $E_a$  within the range 53.16-1836.07 keV.

The resulting  $k_{\epsilon}$  function computed by (11) and the corresponding relative expanded ( $k = 2$ ) uncertainty,  $U_r(k_{\epsilon})$ , versus  $E_a$  computed by (13) of [5] are plotted within the range 59.54-1115.54 keV in Figure 6a and Figure 6b, respectively. Parameters  $A_1, A_2, A_3, A_4, A_5, A_6, B_1, B_2, B_4, B_5$  and  $B_6$ , and their covariance matrixes were used by setting to zero the correlation between  $A_i$  and  $B_j$ . The correlations affecting counting efficiencies  $\epsilon_{\text{std}}(E_m)$  and  $\epsilon_{\text{sm}}(E_a)$  are removed and replaced with the correlations affecting the parameters of the mathematical functions (8) and (9) adopted to model  $k_{\epsilon}$ .

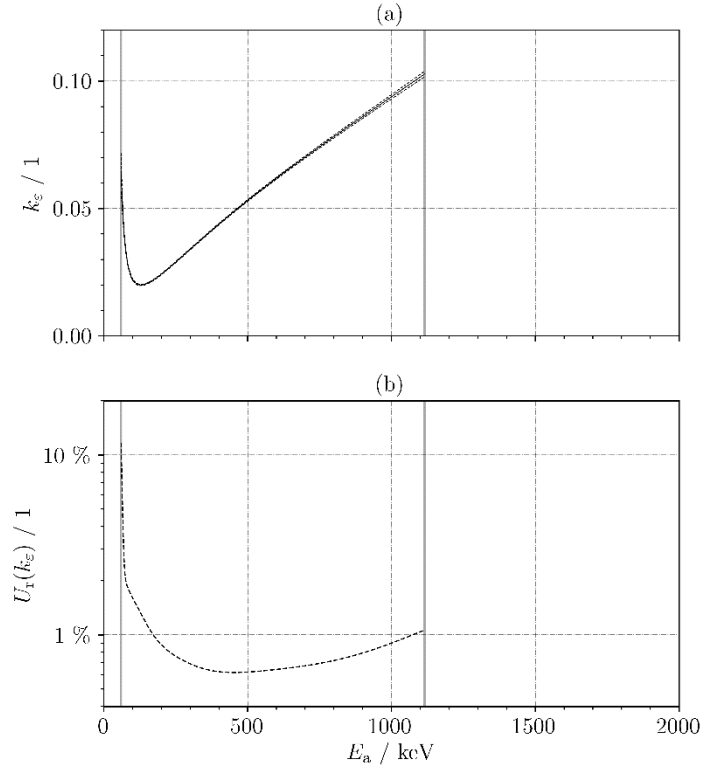


**Figure 6** The  $k_\varepsilon$  function for the determination of a nonspecific analyte in a sample performed by counting  $\gamma$ -photons emitted at energy  $E_a$  using the  $^{198}\text{Au}$  411.8 keV  $E_m$   $\gamma$ -emission as a monitor in a standard (a) and the corresponding relative expanded ( $k = 2$ ) uncertainty,  $U_T(k_\varepsilon)$ , (b) within the range 59.54-1115.54 keV in a double-counting position setup with sample and standard located at 2 cm and 18 cm from the detector end-cap, respectively.

The  $U_T(k_\varepsilon)$  value changes from 10% to 1% within the range 59.54-200 keV and is below 1% within the range 200-1115.54 keV. The sharp increase observed approaching the lower limit of the range is due to the uncertainty of  $k_{\varepsilon\Delta E}$ .

It is worth to note that  $k_\varepsilon$  does not take account the effect of sample and standard measurement at their actual counting positions, modelled in (1) by the ratio  $\frac{(1-\delta\varepsilon_{rm}\delta d_m)}{(1-\delta\varepsilon_{ra}\delta d_a)}$ . This effect becomes significant when the sample counting is performed close to the detector end-cap. Tens of percent relative error might be reached in worst cases and the resultant uncertainty might be a significant contributor to the combined uncertainty of  $w_a$ .

## Conclusion

A method based on the use of reference  $\gamma$ -sources to determine detection efficiency ratios was described to deal with correlations affecting  $\gamma$  counting efficiencies. Its application in analytical chemistry measurements carried out by  $k_0$ -NAA is innovative and offers the possibility to evaluate the uncertainty in agreement with the GUM recommendations in case of correlated input quantities.

Counting efficiencies are redefined in terms of fitted function parameters whose variances and covariances are directly made available in least-square fits of data collected with reference  $\gamma$ -sources at sample and

standard positions. As a result, explicit knowledge of the correlation between counting efficiencies is no longer necessary to evaluate the combined uncertainty of the ratio.

The proposed method requires the adoption of a measurement model slightly different from the largely used classical formulation. Specifically, the effective solid angle was replaced by parameters accounting for extended source geometries and  $\gamma$  self-absorption. As well, the difference between actual and calibrated counting positions is considered to evaluate the effect of the unknown vertical distance between sample and standard.

A detection system was characterized in the case of double-counting setups where standards are located at 18 cm from the detector end-cap and samples at different distances ranging from 2 cm to 16 cm with 2 cm steps. In the worst case, i.e. when the small amount of the investigated analyte requires the closest distance sample position for its quantification, the uncertainty of the detection efficiency ratio can be limited at sub-percent level.

Nevertheless, the experimental flexibility is limited when extended sources are measured because corrections for geometry and  $\gamma$  self-absorption reach tens of percent levels. Specific determinations of the effects are theoretically possible by preparing and using extended reference  $\gamma$ -sources.

Albeit the low uncertainty reached is already suitable for trace analysis, the extension of the  $\gamma$ -energy range using additional calibration efficiency values measured with true-coincidence free  $\gamma$  emissions at higher energy is essential. Moreover, the routine application in  $k_0$ -NAA requires extensive testing in measurement campaigns carried out in different experimental conditions with certified reference materials, e.g. Synthetic Multi-element Standards [15].

## References

- [1] Révay, Z, Kennedy G; "Application of the  $k_0$  method in neutron activation analysis and in prompt gamma activation analysis", *Radiochim Acta* **2012**; 100, 687-698
- [2] Milton M J T, Quinn T J; "Primary methods for the measurement of amount of substance", *Metrologia* **2001**; 38, 289-296
- [3] Révay Z, Belgia T; "Principles of PGAA" In: "Prompt Gamma Activation Analysis with Neutron Beams" (Molnar, G.L., ed.) *Kluwer Academic Publishers*, Dordrecht, **2004**; p.1
- [4] De Corte F; "The  $k_0$ -standardization method, a move to the optimization of neutron activation analysis", Habilitation Thesis, University of Gent, Belgium, **1987**
- [5] "Guide to the expression of Uncertainty in Measurement" (GUM JCGM 100:2008), *International Organization for Standardization*, **2008**
- [6] Molnar G L, Révay Z, Belgia T; "Wide energy range efficiency calibration method for Ge detectors", *Nucl Instrum Methods Phys Res A*, **2002**; 489, 140-159
- [7] Révay Z; "Calculation of uncertainties in prompt gamma activation analysis", *Nucl Instrum Methods Phys Res A*, **2006**; 564, 688-697

- [8] Belgya T; "Uncertainty calculation of functions of  $\gamma$ -ray detector efficiency and its usage in comparator experiments", *J Radioanal Nucl Chem*, **2014**; 300, 559-566
- [9] Punte L R M, Lalremruata B, Otuka N, Suryanarayana S V, Iwamoto Y, Pachua R, Satheesh B, Thanga H H, Danu L S, Desai V V, Hlondo L R, Kailas S, Ganesan S, Nayak B K, Saxena A; "Measurements of neutron capture cross sections on  $^{70}\text{Zn}$  at 0.96 and 1.69 MeV", *Phys Rev C* 95, **2017**; 95, 024619
- [10] Otuka N, Lalremruata B, Khandaker M U, Usman A R, Punte L R M; "Uncertainty propagation in activation cross section measurements", *Radiat Phys Chem*, **2017**; 140, 502-510
- [11] D'Agostino G, Di Luzio M, Oddone M; "An uncertainty spreadsheet for the  $k_0$ -standardization method in Neutron Activation Analysis", *J Radioanal Nucl Chem*, **2018**; 318, 1261-1269
- [12] D'Agostino G, Di Luzio M, Oddone M; "The  $k_0$ -INRIM software: a tool to compile uncertainty budgets in Neutron Activation Analysis based on  $k_0$ -standardisation", *Meas Sci Technol*, **2020**; Accepted, DOI: [10.1088/1361-6501/ab358f](https://doi.org/10.1088/1361-6501/ab358f)
- [13] Gilmore G; "Practical gamma-ray spectrometry", *Wiley*, Second Edition, **2008**
- [14] Nudat 2, <https://www.nndc.bnl.gov/nudat2/>
- [15] Vermaercke P, Robouch P, Eguskiza M, De Corte F, Kennedy G, Smodiš B, Jaćimović R, Yonezawa C, Matsue H, Lin X, Blaauw M, Kučera J; "Characterization of Synthetic Multi-element Standards (SMELS) Used for the Validation of  $k_0$ -NAA", *Nucl Instrum Methods Phys Res A*, **2006**; 564, 675-682